

Table II. Correlation for the Intramolecular Vibrations of NO_2^+ and NO_3^- in the $\text{NO}_2^+\text{NO}_3^-$ Crystal between Their Point Groups, Site Groups, and Factor Groups and Their Infrared and Raman Activities

	approx description of mode	point group	site group	factor group
NO_3^-	symm str	D_{3h}	D_{3h}	D_{6h}
		$A_1'(\text{R})$	$A_1'(\text{R})$	$A_{1g}(\text{R})$
	out-of-plane def	$A_2''(\text{IR})$	$A_2''(\text{IR})$	$B_{1u}(\text{IR})$
				$A_{2u}(\text{IR})$
antisymm str	$E'(\text{R, IR})$	$E'(\text{R, IR})$	$B_{2g}(\text{R})$	
			$E_{1u}(\text{IR})$	
in-plane def	$E'(\text{R, IR})$	$E'(\text{R, IR})$	$E_{2g}(\text{R})$	
			$E_{1u}(\text{IR})$	
NO_2^+	symm str	D_{3h}	D_{3d}	D_{6h}
		$\Sigma_g^+(\text{R})$	$A_{1g}(\text{R})$	$A_{1g}(\text{R})$
	antisymm str	$\Sigma_u^+(\text{IR})$	$A_{2u}(\text{IR})$	$A_{2u}(\text{IR})$
				$B_{1u}(\text{IR})$
def	$\Pi_u(\text{IR})$	$E_u(\text{IR})$	$E_{1u}(\text{IR})$	
			$E_{2u}(\text{IR})$	
	$2 \times \text{def } (D_{6h})$			
	$2E_{1u} = A_{1g} + A_{2g} + E_{2g}(\text{R})$			
	$2E_{2u} = A_{1g} + A_{2g} + E_{2g}(\text{R})$			
	$E_{1u} \cdot E_{2u} = B_{1g} + B_{2g} + E_{1g}(\text{R})$			

recorded. The observed spectrum (see Figure 1 and Table I) exhibited more bands than previously reported^{13,14} and predicted from the known crystal structure¹⁶ and a factor group analysis (see Table II). To verify that these additional Raman bands belonged indeed to N_2O_5 , a sample of N_2O_5 was also prepared from N_2O_4 and ozone and its Raman spectrum was recorded. The observed spectrum was identical with that of Figure 1.

According to the previous X-ray crystal study,¹⁶ N_2O_5 crystallizes in the space group D_{6h}^4 ($C6/mmc$) with $Z = 2$ and trigonal-planar NO_3^- anions in D_{3h} sites and linear symmetric NO_2^+ cations in D_{3d} sites. The structure was based on 64 nonzero reflections with a final R value of 0.120. The refinement of this structure was subsequently confirmed by Cruickshank and co-workers but raised a question concerning the bond lengths of the NO_2^+ cations in $\text{NO}_2^+\text{NO}_3^-$ and $\text{NO}_2^+\text{ClO}_4^-$. Although the symmetric NO_2^+ stretching modes are practically identical in both compounds, the bond lengths differed by 0.049 Å and rotational oscillation corrections were suggested as a possible explanation for this large discrepancy.²¹

If we return to the Raman spectrum of solid N_2O_5 , the only two previous studies^{13,14} were carried out with Toronto arc excitation. Only two Raman lines at about 1400 and 1050 cm^{-1} were observed and correctly attributed to the symmetric NO_2^+ and NO_3^- stretching modes, respectively. We have now also observed (see Figure 1 and Table I) the antisymmetric stretch and the in-plane deformation modes for NO_3^- at 1350 and 722 cm^{-1} , respectively, and the deformation mode for NO_2^+ at 534 cm^{-1} . Whereas the Raman activity of ν_{as} and $\delta_{\text{in plane}}$ of NO_3^- is in accord with the results of the factor group analysis (see Table II), the latter cannot explain the intense Raman band observed for the NO_2^+ deformation mode.

The Raman and infrared activities and relative intensities of the NO_2^+ modes in $\text{NO}_2^+\text{NO}_3^-$ closely resemble those in $\text{NO}_2^+\text{ClO}_4^-$,²² which contains a slightly bent ($\angle\text{ONO} = 175.2 \pm 1.4^\circ$) NO_2^+ cation.²¹ Our data for $\text{NO}_2^+\text{NO}_3^-$, therefore, suggest that the NO_2^+ cation in solid N_2O_5 might be similarly bent. The failure of the X-ray crystal structure study to detect this nonlinearity of NO_2^+ for $\text{NO}_2^+\text{NO}_3^-$ might be attributed to facts such as the low precision of the X-ray study (64 reflections, $R = 0.12$)¹⁶ or, more likely, rotational oscillation of the NO_2^+ cation,²¹ which could result in an averaged linear structure for a slightly nonlinear ion. Such an averaging would not be observable on the vibrational spectroscopy time scale.

In addition to the above discussed fundamental vibrations, several very weak bands were observed in the Raman spectrum

of solid $\text{NO}_2^+\text{NO}_3^-$. The three bands at 1087, 1079, and 1065 cm^{-1} can be attributed to the first overtone of the NO_2^+ deformation mode in Fermi resonance with the symmetric stretching mode. The splitting into three components can be explained by the assumption of an E_{2u} component for the deformation mode that is inactive in both the infrared and Raman spectra but whose overtone and combination bands are Raman active (see Table II). The weak band at 687 cm^{-1} is attributed to a combination band of the NO_2^+ deformation with the 161- cm^{-1} lattice mode. For the very weak band at 1028 cm^{-1} we do not have, at the present time, a plausible explanation.

Acknowledgment. The authors thank Drs. C. J. Schack and L. R. Grant and R. D. Wilson for their help and the U.S. Army Research Office and the Office of Naval Research for financial support.

Contribution from the Department of Chemistry,
University of Oklahoma, Norman, Oklahoma 73019

Preparation and Molecular Structure of $\text{OMo}^{\text{IV}}[\text{S}_2\text{C}_2(\text{CN})_2](\text{Ph}_2\text{PCH}_2\text{CH}_2\text{PPh}_2) \cdot (\text{CH}_3)_2\text{CO}$ and Its Possible Relevance to the Active Site of Oxo-Transfer Molybdoenzymes

Kenneth M. Nicholas* and Masood A. Khan

Received October 27, 1986

The apparent role of oxo-type molybdenum centers in various enzymatic redox processes has stimulated exploration of the structural, spectroscopic, and reactivity features of higher oxidation state molybdenum compounds as well as efforts to construct models for these molybdoenzymes. A combination of EXAFS, EPR, electrochemical, chemical modeling, and microbiological studies on these oxidoreductases (e.g. sulfite, xanthine, and CO oxidases and nitrate reductase) has led to the widely held belief that these enzymes contain a common cofactor in which the Mo atom shuttles between the Mo(IV) and Mo(VI) states and has at least one oxo and two S-donor ligands (e.g. thiolate).¹

On the basis of recent chemical degradation studies of the molybdenum cofactor ($\text{Mo}(\text{co})$) from xanthine and sulfite oxidases,

(21) Truter, M. R.; Cruickshank, D. W. J.; Jeffrey, G. A. *Acta Crystallogr.* **1960**, *13*, 855.

(22) Nebgen, J. W.; McElroy, A. D.; Klodowski, H. F. *Inorg. Chem.* **1965**, *4*, 1796.

(1) Reviews: Burgmayer, S. J. N.; Stiefel, E. I. *J. Chem. Educ.* **1985**, *62*, 943. *Molybdenum and Molybdenum-Containing Enzymes*; Coughlan, M. P., Ed.; Pergamon: New York, 1980. *Molybdenum Chemistry of Biological Significance*; Newton, W. E., Otsuka, S., Eds.; Plenum: New York, 1980.

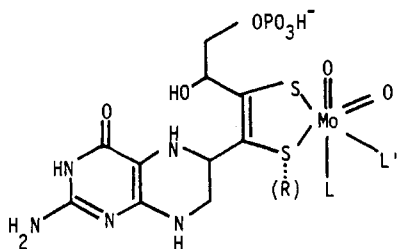
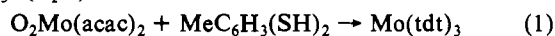


Figure 1. Proposed structure for Mo(co) (in oxidized form).

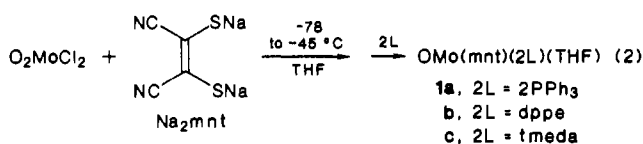
Rajagopalan and co-workers made the intriguing suggestion that the Mo coordination sphere includes a pterin-derived *dithiolene* (Figure 1).² Although the correctness of this formulation remains to be demonstrated, it is interesting nonetheless on a number of accounts. First, while metal-dithiolene complexes have a rich history in structural coordination chemistry,³ their biological relevance previously had not been considered. However, the ability of the dithiolene ligand to stabilize multiple metal oxidation states⁴ could enable dithiolene complexes to function as versatile redox catalysts. Curiously, mixed ligand-dithiolene complexes are rather uncommon and only one, partly characterized, example of an oxo-dithiolene species, OMo(mnt)₂²⁻, has been reported⁵ (mnt = S₂C₂(CN)₂). We have sought, therefore, to prepare O_xMo(dithiolene)L_y complexes (*x* = 1, 2; *y* = 2, 3) in order to explore their fundamental chemistry and suitability as structural and functional models for the active site of oxo-transfer molybdoenzymes. Our preliminary findings are reported herein.

Results and Discussion

Our initial efforts using 3,4-toluenedithiol (tdtH₂) were discouraging. Thus, treatment of O₂Mo(acac)₂ (acac = acetylacetonate) with 1 equiv of tdtH₂ in the presence of L = DMF or pyridine even at -78 °C led to rapid formation of green-blue Mo(tdt)₃⁵ (eq 1).



On the other hand, when MoO₂Cl₂ in THF is treated with Na₂S₂C₂(CN)₂ (Na₂mnt) at -78 to -45 °C, an orange mixture is formed. Although warming of this mixture above -45 °C also results in the production of a totally deoxygenated product, blue Na₂Mo(mnt)₃⁵ if the system is maintained at low temperature followed by addition of suitable ligands, i.e. PPh₃, Ph₂PCH₂CH₂PPh₂ (dppe), and Me₂N(CH₂)₂NMe₂ (tmeda), the stable adducts **1a-c** can be isolated in moderate yield (eq 2).



Preliminary spectroscopic evaluation of these species indicated the simultaneous presence of the oxo group ($\nu(\text{Mo}=\text{O}) = 925\text{--}975 \text{ cm}^{-1}$), mnt ($\nu(\text{C}\equiv\text{N}) = 2200\text{--}2210 \text{ cm}^{-1}$), and the added ligand L and THF (for **1a,b**; by ¹H NMR).

In order to confirm the above hypothesis and to establish the stoichiometries and detailed structures of these complexes, we obtained crystals of the dppe adduct from acetone solution (**2b**) and performed an X-ray diffraction study. The X-ray structure of **2b** is shown in Figure 2; important bond angles and lengths are given in Table III. This tetragonally distorted pseudooctahedral structure may be viewed alternatively as a capped square-pyramidal arrangement about Mo(IV) with mnt and dppe

Table I. Crystal Data for OMo(dppe)(mnt)-(CH₃)₂CO (**2b**)

formula	C ₃₃ H ₃₀ MoN ₂ O ₂ P ₂ S ₂
fw	708.63
temp for data collec and cell const	138 ± 2 K
cell const ^a	<i>a</i> = 18.580 (5) Å, <i>b</i> = 14.943 (8) Å, <i>c</i> = 11.391 (4) Å, β = 90.75 (3)°
<i>V</i>	3162 Å ³
space group	<i>P</i> 2 ₁ / <i>n</i> (nonstd setting of <i>P</i> 2 ₁ / <i>c</i>)
<i>Z</i>	4
<i>d</i> _{calcd} at 138 ± 2 K	1.488 g cm ⁻³
radiation (monochromated)	Mo Kα (λ = 0.710 69 Å)
μ(Mo Kα)	6.03 cm ⁻¹
cryst size	0.45 × 0.18 × 0.18 mm
scan type	ω-2θ
data collec range, 2θ	3-50°
total reflcns measd (± <i>h,k,l</i>)	5795
unique data used (<i>I</i> > 2σ(<i>I</i>))	4572
<i>R</i> = Σ <i>F</i> _o - <i>F</i> _c / Σ <i>F</i> _o	0.031
<i>R</i> _w = [Σ <i>w</i> (<i>F</i> _o - <i>F</i> _c) ² / Σ <i>w</i> <i>F</i> _o ²] ^{1/2}	0.032
GOF = [Σ <i>w</i> (<i>F</i> _o - <i>F</i> _c) ² / (<i>m</i> - <i>n</i>)] ^{1/2}	1.75
largest shift/esd, final cycle	0.1
ρ _{max} in the final diff map	0.5 e Å ⁻³

^aCell constants were derived by least-squares analysis of the diffractometer angular setting of 24 well-centered reflections (2θ range 30-40°).

Table II. Final Positional Coordinates of the Non-Hydrogen Atoms of **2b**

atom	<i>x</i>	<i>y</i>	<i>z</i>
Mo	0.29196 (1)	0.52062 (2)	0.32477 (2)
S(1)	0.19820 (4)	0.59205 (5)	0.43526 (6)
S(2)	0.37006 (4)	0.57055 (5)	0.48065 (7)
P(1)	0.37935 (4)	0.40130 (5)	0.25767 (6)
P(2)	0.20821 (4)	0.42097 (5)	0.20502 (6)
O(1)	0.3112 (1)	0.5914 (1)	0.2146 (2)
O(2)	0.2637 (1)	0.3919 (1)	0.4306 (2)
N(1)	0.1683 (2)	0.7582 (2)	0.6701 (3)
N(2)	0.3807 (2)	0.7372 (2)	0.7251 (3)
C(1)	0.3339 (2)	0.3375 (2)	0.1397 (3)
C(2)	0.2565 (2)	0.3162 (2)	0.1746 (3)
C(3)	0.2451 (2)	0.6515 (2)	0.5456 (2)
C(4)	0.2032 (2)	0.7109 (2)	0.6162 (3)
C(5)	0.3169 (2)	0.6432 (2)	0.5644 (3)
C(6)	0.3528 (2)	0.6946 (2)	0.6539 (3)
C(7)	0.2551 (2)	0.3586 (2)	0.5282 (3)
C(8)	0.2420 (2)	0.2604 (3)	0.5391 (3)
C(9)	0.2609 (3)	0.4108 (3)	0.6379 (3)
C(11)	0.4087 (2)	0.3171 (2)	0.3644 (3)
C(12)	0.3972 (2)	0.2258 (2)	0.3494 (3)
C(13)	0.4198 (2)	0.1658 (2)	0.4347 (3)
C(14)	0.4540 (2)	0.1960 (2)	0.5359 (3)
C(15)	0.4668 (2)	0.2864 (2)	0.5498 (3)
C(16)	0.4445 (2)	0.3467 (2)	0.4651 (3)
C(21)	0.4632 (2)	0.4419 (2)	0.1966 (3)
C(22)	0.5035 (2)	0.3906 (2)	0.1202 (3)
C(23)	0.5694 (2)	0.4220 (3)	0.0813 (3)
C(24)	0.5952 (2)	0.5033 (2)	0.1186 (3)
C(25)	0.5556 (2)	0.5544 (3)	0.1947 (3)
C(26)	0.4893 (2)	0.5245 (2)	0.2331 (3)
C(31)	0.1236 (2)	0.3881 (2)	0.2709 (3)
C(32)	0.1055 (2)	0.2994 (2)	0.2952 (3)
C(33)	0.0420 (2)	0.2806 (3)	0.3529 (3)
C(34)	-0.0034 (2)	0.3486 (3)	0.3852 (3)
C(35)	0.0129 (2)	0.4362 (3)	0.3603 (3)
C(36)	0.0766 (2)	0.4562 (2)	0.3030 (3)
C(41)	0.1824 (2)	0.4576 (2)	0.0572 (3)
C(42)	0.1224 (2)	0.4208 (2)	0.0015 (3)
C(43)	0.1032 (2)	0.4464 (3)	-0.1116 (3)
C(44)	0.1441 (2)	0.5087 (2)	-0.1703 (3)
C(45)	0.2050 (2)	0.5443 (2)	-0.1171 (3)
C(46)	0.2238 (2)	0.5200 (2)	-0.0031 (3)

ligands in the basal plane, the oxo ligand in the apical position, and the acetone molecule capping the position trans to the oxo ligand. This model is supported by the location of the Mo atom 0.4233 (3) Å above the S,S,P,P plane. While this value is below

- Johnson, J. L.; Hainline, B. E.; Rajagopalan, K. V. *J. Biol. Chem.* **1980**, *255*, 1783. Johnson, J. L.; Hainline, B. E.; Rajagopalan, K. V.; Arison, B. H. *J. Biol. Chem.* **1984**, *259*, 5414.
- Reviews: McCleverty, J. A. *Prog. Inorg. Chem.* **1968**, *10*, 145. Schrauzer, G. N. *Acc. Chem. Res.* **1969**, *2*, 72. Eisenberg, R. *Prog. Inorg. Chem.* **1970**, *12*, 295. Stiefel, E. I. *Prog. Inorg. Chem.* **1977**, *22*, 154-159.
- Wharton, E. J.; McCleverty, J. A. *J. Chem. Soc. A* **1969**, 2258.
- Stiefel, E. I.; Bennett, L. E.; Dori, Z.; Crawford, T. H.; Simo, C.; Gray, H. B. *Inorg. Chem.* **1970**, *9*, 281.

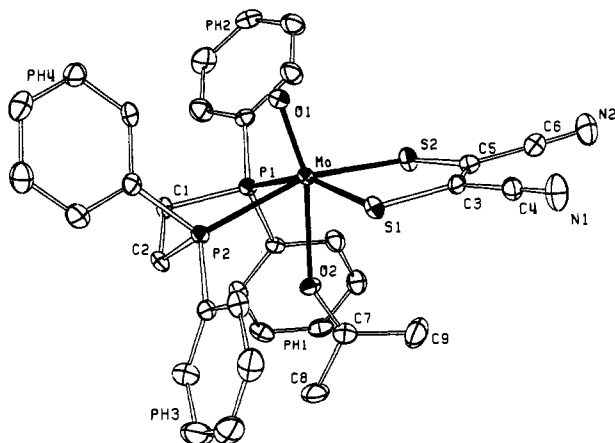


Figure 2. Perspective view of **2b**. Thermal ellipsoids are shown at the 50% level. Hydrogen atoms are omitted for clarity. The numbering scheme for the phenyl carbon atoms is C(*mn*) (*m* = 1–4, *n* = 1–6).

Table III. Selected Bond Lengths (Å) and Angles (deg) for **2b**

(a) Bond Lengths			
Mo–S(1)	2.412 (1)	P(2)–C(31)	1.818 (3)
Mo–S(2)	2.397 (1)	P(2)–C(41)	1.829 (3)
Mo–P(1)	2.536 (1)	O(2)–C(7)	1.231 (4)
Mo–P(2)	2.538 (1)	N(1)–C(4)	1.144 (4)
Mo–O(1)	1.682 (2)	N(2)–C(6)	1.149 (4)
Mo–O(2)	2.333 (2)	C(1)–C(2)	1.530 (4)
S(1)–C(3)	1.762 (3)	C(3)–C(4)	1.434 (4)
S(2)–C(5)	1.757 (3)	C(3)–C(5)	1.354 (4)
P(1)–C(1)	1.844 (3)	C(5)–C(6)	1.435 (4)
P(1)–C(11)	1.828 (3)	C(7)–C(8)	1.493 (5)
P(1)–C(21)	1.818 (3)	C(7)–C(9)	1.476 (5)
P(2)–C(2)	1.840 (3)		
(b) Bond Angles			
S(1)–Mo–S(2)	84.8 (1)	Mo–P(2)–C(2)	107.7 (1)
S(1)–Mo–P(1)	159.7 (1)	Mo–P(2)–C(31)	117.7 (1)
S(1)–Mo–P(2)	95.6 (1)	Mo–P(2)–C(31)	118.7 (1)
S(1)–Mo–O(1)	105.8 (1)	C(2)–P(2)–C(31)	105.9 (1)
S(1)–Mo–O(2)	85.8 (1)	C(2)–P(2)–C(41)	101.8 (1)
S(2)–Mo–P(1)	93.3 (1)	C(31)–P(2)–C(41)	104.1 (1)
S(2)–Mo–P(2)	160.3 (1)	Mo–O(2)–C(7)	146.4 (2)
S(2)–Mo–O(1)	103.0 (1)	P(1)–C(1)–C(2)	110.0 (2)
S(2)–Mo–O(2)	90.7 (1)	P(2)–C(2)–C(1)	109.5 (2)
P(1)–Mo–P(2)	79.4 (1)	S(1)–C(3)–C(4)	116.4 (2)
P(1)–Mo–O(1)	94.3 (1)	S(1)–C(3)–C(5)	122.9 (2)
P(1)–Mo–O(2)	74.1 (1)	C(4)–C(3)–C(5)	120.7 (3)
P(2)–Mo–O(1)	95.9 (1)	C(3)–C(4)–N(1)	178.0 (3)
P(2)–Mo–O(2)	69.7 (1)	S(2)–C(5)–C(3)	122.1 (2)
O(1)–Mo–O(2)	162.7 (1)	S(2)–C(5)–C(6)	117.3 (2)
Mo–S(1)–C(3)	104.0 (1)	C(3)–C(5)–C(6)	120.6 (3)
Mo–S(2)–C(5)	104.8 (1)	C(5)–C(6)–N(2)	178.8 (4)
Mo–P(1)–C(1)	107.1 (1)	O(2)–C(7)–C(8)	119.8 (3)
Mo–P(1)–C(11)	118.0 (1)	O(2)–C(7)–C(9)	122.8 (3)
Mo–P(1)–C(21)	115.8 (1)	C(8)–C(7)–C(9)	117.4 (3)
C(1)–P(1)–C(11)	105.0 (1)		
C(1)–P(1)–C(21)	106.3 (1)		
C(11)–P(1)–C(21)	103.6 (1)		

the 0.71–0.86-Å range of representative five-coordinate $\text{OMo}^{\text{IV}}\text{L}_4$ species,⁶ it is the largest displacement yet observed for any six-coordinate $\text{OMo}^{\text{IV}}\text{L}_4\text{-L}'$ complex (0.0–0.33 Å).⁷ The apparent correlation of this distance with the strength of the M–L' bond,^{7a} together with the rather long Mo–O–OCMe₂ distance (2.333 (2) Å),⁸ is suggestive of a weak Mo–acetone interaction and may

presage enhanced substitutional lability for this and other ligands occupying the position trans to the oxo ligand.^{9,10} It is interesting to note that while the bond lengths of the coordinated acetone in **2b** are essentially the same as for uncoordinated acetone,¹¹ the $\nu(\text{C}=\text{O})$ band at 1660 cm^{-1} is considerably lowered (ca. 60 cm^{-1}). All the other Mo–L bond lengths (L = O, S, P) are normal as are the distances within the mnt and dppe ligands. The distortion of the O–Mo–O “axis” away from the mnt ligand is quite pronounced (O(1)–Mo–O(2) = 162.7 (1)°; the angles of the Mo–O(1) and Mo–O(2) vectors from the S,S,P,P plane are 83.8 (5) and 78.1 (4)°, respectively) and is especially interesting because it is apparently contrasteric. Presently, we have no explanation for this effect as there are no unusually short intermolecular contacts.¹²

Since the final products of eq 2 are Mo(IV) derivatives, it is obvious that the starting Mo(VI) species undergoes reduction. Either mnt²⁻ or phosphine could serve this role,^{13,14} but this issue has not yet been settled experimentally.

We have briefly surveyed the reactivity of $\text{OMo}(\text{mnt})(\text{dppe})\cdot\text{THF}$ (**1b**) toward added prospective ligands and oxidants. Solutions of **1b** in THF showed no change (monitored by UV/vis) when treated with CO, maleic anhydride, DMF, or pyridine, but addition of 1–10 equiv of the secondary amine morpholine (morph) caused rapid disappearance of the starting complex and appearance of new bands at 350, 310, and 250 nm, which we ascribe tentatively to $\text{OMo}(\text{mnt})(\text{dppe})\cdot\text{morph}$. **1a,b** also react readily with O-transfer oxidants such as Me₃NO and *m*-ClC₆H₄CO₃H. Efforts are under way to isolate and characterize the expected $\text{O}_2\text{Mo}^{\text{VI}}(\text{mnt})\text{L}_2$ products.

The feasibility of coexistent oxo and dithiolene ligands on the same metal center has thus been firmly established. The relevance of this feature to the structure of Mo(co) remains to be determined through future synthetic, spectral, and chemical studies.

Experimental Section

General Considerations. All reactions and manipulations were carried out under an atmosphere of prepurified nitrogen with use of standard Schlenk and drybox techniques. Tetrahydrofuran and benzene were distilled from Na/benzophenone, and acetone was distilled from boric oxide. MoO₂Cl₂ and 3,4-toluenedithiol were obtained commercially. Na₂mnt²⁻ and MoO₂(acac)₂¹⁵ were prepared by using literature methods.

Preparation of $\text{OMo}(\text{mnt})\text{L}_2\cdot\text{THF}$. The same general method was employed for the complexes L = PPh₃ and L₂ = dppe, tmeda. A 50-mL side-arm round-bottom flask was charged with 0.40 g (2.0 mmol) of MoO₂Cl₂, 20 mL of dry THF, and a magnetic stirring bar (in the drybox). The solution was then cooled to –78 °C, and 0.38 g (2.0 mmol) of Na₂mnt was added in one portion under a nitrogen flush. After it was

(6) Ricard, L.; Estienne, J.; Karagiannidis, P.; Toledano, P.; Fischer, J.; Mitschler, A.; Weiss, R. *J. Coord. Chem.* **1974**, *3*, 277. Hyde, J.; Venkatasubramanian, K.; Zubieta, J. *Inorg. Chem.* **1978**, *17*, 414. Draganjac, M.; Simhon, E.; Chan, L. T.; Kanatzidis, M.; Baenziger, N.; Coucouvanis, D. *Inorg. Chem.* **1982**, *21*, 3321. Mennemann, K.; Mattes, R. *J. Chem. Res., Miniprint* **1979**, 1372.

(7) (a) Lam, C. T.; Lewis, D. L.; Lippard, S. *Inorg. Chem.* **1976**, *15*, 989. (b) Bishop, M. W.; Chatt, J.; Dilworth, J. R.; Hursthouse, M. B.; Matevalli, M. *J. Chem. Soc., Dalton Trans.* **1979**, 1603.

(8) Second- and third-row transition-metal–acetone M–O distances in the range of 2.07–2.24 Å have been reported; e.g. Ru–O = 2.194 (8) Å (Gould, R. O.; Sime, W. J.; Stephenson, T. A. *J. Chem. Soc., Dalton Trans.* **1978**, 76), Ir–O = 2.235 (5) Å (Crabtree, R. H.; Hlatky, G. G.; Parnell, C. P.; Segmuller, B. E.; Uriarte, R. *J. Inorg. Chem.* **1984**, *23*, 354), Pt–O = 2.167 (4) Å Thayer, A. G.; Payne, N. C. *Acta Crystallogr., Sect. C: Cryst. Struct. Commun.* **1986**, *C42*, 1302), and Re–O = 2.07 Å (Gladysz, J., to be submitted for publication).

(9) A similarly long Mo–O length (2.382 (3) Å) for a Mo–OSMe₂ linkage trans to the oxo ligand has recently been found by Holm and Berg; Berg, J. M.; Holm, R. H. *J. Am. Chem. Soc.* **1985**, *107*, 917.

(10) A similar ability of square-pyramidal $\text{OMe}(\text{S,CNR})_2$ to accommodate ligands trans to the oxo ligand has been observed: Schneider, P. W.; Bravard, D. C.; McDonald, J. W.; Newton, W. E. *J. Am. Chem. Soc.* **1972**, *94*, 8640. Ricard, L.; Weiss, R. *Inorg. Nucl. Chem. Lett.* **1974**, *10*, 217.

(11) (a) Allen, P. W.; Bowen, H. J. M.; Sutton, L. E.; Bastiansen, O. *Trans. Faraday Soc.* **1952**, *48*, 991. (b) di Vaira, M.; Stoppioni, P.; Mani, F. *J. Organomet. Chem.* **1983**, *247*, 95.

(12) A reviewer has suggested that this distortion may be the result of repulsion between the oxo and dithiolene donor atoms as is found in the theoretical analysis of $\text{MoO}_2(\text{SH})_2(\text{NH}_3)_2$ structures: Holm, R. H.; Berg, J. M. *Pure Appl. Chem.* **1984**, *56*, 1645.

(13) The oxidation of mnt²⁻ has been studied: Simmons, H. E.; Blomstrom, D. C.; Vest, R. D. *J. Am. Chem. Soc.* **1962**, *84*, 4756.

(14) References to reduction of $\text{O}_2\text{Mo}^{\text{VI}}\text{L}_2$ by phosphines: Newton, W. E.; Corbin, J. C.; Bravard, D. C.; Searles, J. E.; McDonald, J. W. *Inorg. Chem.* **1974**, *13*, 1000. Berg, J. M.; Holm, R. H. *J. Am. Chem. Soc.* **1985**, *107*, 925.

(15) Jones, M. M. *J. Am. Chem. Soc.* **1959**, *81*, 3188.

stirred for approximately 1 h (at $-78\text{ }^{\circ}\text{C}$), the mixture was orange. At this time the selected ligand was added (2.0 mmol) and the resulting mixture was allowed to warm slowly to room temperature with stirring. The mixture was filtered, and the resulting filtrate was concentrated in vacuo to leave the crude product complex as a burgundy solid (PPh_3 and dppe adducts) or a yellow oil (tmeda adduct). These were washed with several portions of dry benzene to remove any excess ligand present and dried under vacuum (40–50% yield). Attempts to obtain analytically pure samples of the PPh_3 and tmeda adducts by recrystallization or chromatography (decomposition on alumina, silica gel, Florisil) were unsuccessful. Spectral properties of these products follow.

OMo(mnt)(PPh_3) $_2$ ·THF (1a): IR (KBr) 2200 ($\nu(\text{CN})$), 960 ($\nu(\text{MoO})$) cm^{-1} ; UV/vis (THF) 500, 400, 320, 250 nm; ^1H NMR (acetone- d_6) δ 7.0–8.0 (m, C_6H_5), 3.6 (t, OCH_2), 1.8 (m, CH_2CH_2).

OMo(mnt)(dppe)·THF (1b): IR (KBr) 2200 ($\nu(\text{CN})$), 970 ($\nu(\text{MoO})$) cm^{-1} ; UV/vis (THF) 530, 450, 400, 315, 250 nm; ^1H NMR (acetone- d_6) δ 7.2–8.0 (m, C_6H_5), 3.6 (t, OCH_2), 3.4 (t, PCH_2), 3.05 (m, PCH_2), 1.8 (m, CH_2CH_2).

OMo(mnt)(tmeda) (1c): IR (KBr) 2200 ($\nu(\text{CN})$), 925 ($\nu(\text{MoO})$) cm^{-1} ; UV/vis (THF) 425, 360, 280, 250 nm; ^1H NMR (acetone- d_6) δ 3.1 (s, 4 H, NCH_2), 2.6 (s, 6 H, NCH_3); ^{13}C NMR (acetone- d_6) δ 53.9, 43.9.

Crystal Structure of OMo(mnt)(dppe)-(CH $_3$) $_2$ CO (2b). Deep red crystals of **2b** were obtained when **1b** was dissolved in acetone and let stand overnight under N_2 . The crystal selected was mounted on a glass fiber, and the data were collected on an Enraf-Nonius CAD-4 diffractometer by the methods standard in this laboratory.¹⁶ The data were corrected for Lorentz and polarization effects; no absorption correction was applied since it was judged to be negligible. The structure was solved by the heavy-atom method and refined by least squares (SHELX-76)¹⁷ minimizing $\sum w(|F_o| - |F_c|)^2$. Positional and anisotropic thermal parameters were refined for all the non-hydrogen atoms in two blocks. Only the methyl hydrogen atoms were refined isotropically, while all the other hydrogen atoms were included in the idealized positions ($\text{C-H} = 0.95\text{ \AA}$).

The atomic scattering factors were taken from ref 18. Data pertaining to data collection and refinement are summarized in Table I. Table II lists the atomic coordinates, and selected bond lengths and angles are given in Table III.

Supplementary Material Available: Listings of hydrogen atom coordinates, anisotropic thermal parameters, and supplementary bond lengths and angles (6 pages); a table of calculated and observed structure factors (20 pages). Ordering information is given on any current masthead page.

(16) Hossain, M. B.; van der Helm, D.; Poling, M. *Acta Crystallogr., Sect. B: Struct. Sci.* **1983**, *B39*, 258.

(17) Sheldrick, G. M. *Computing in Crystallography*; Delft University Press: Delft, The Netherlands, 1978; pp 34–42.

(18) *International Tables for X-ray Crystallography*; Kynoch: Birmingham, England, 1974; Vol. IV, pp 99, 149.

Contribution from the School of Chemical Sciences,
University of Illinois at Urbana-Champaign,
Urbana, Illinois 61801, and Department of Chemistry,
University of Delaware, Newark, Delaware 19716

Ditellurene, Selenatellurene, and Thiatellurene Complexes. The Structure of Pt(1,2- $\text{Te}_2\text{C}_6\text{H}_4$)(PPh_3) $_2$

Dean M. Giolando,[†] Thomas B. Rauchfuss,^{*†}
and Arnold L. Rheingold^{*†}

Received September 3, 1986

Metal complexes formally derived from alkenedichalcogenides or 1,2-benzenedichalcogenides have been heavily studied for more than 20 years.¹ Best known of these ligand types are the sulfur derivatives (dithiolenes) although recent work has focused on the selenium analogues (diselenenes).² Interest in this class of chelating ligands continues to grow, particularly with regard to

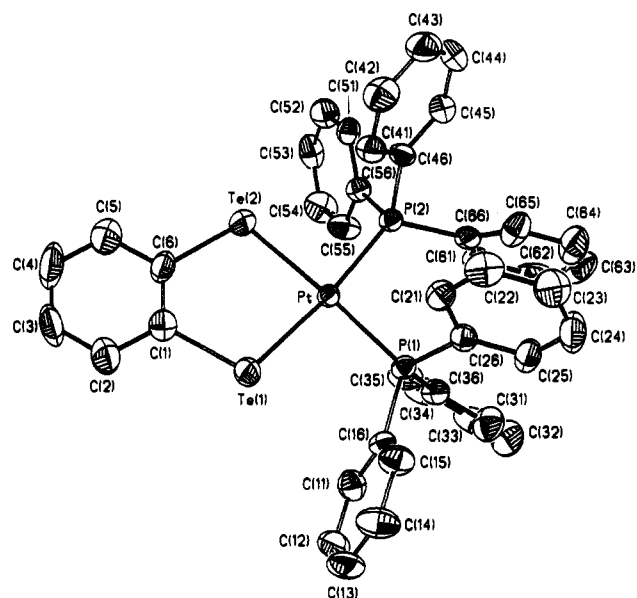


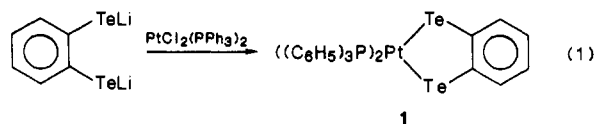
Figure 1. ORTEP plot of $\text{Pt}(\text{Te}_2\text{C}_6\text{H}_4)(\text{PPh}_3)_2$ (**1**).

their applications in materials science.^{3,4} Large and highly polarizable main-group centers in alkenedichalcogenide complexes should enhance the intermolecular electronic coupling leading to the formation of conduction bands. It is the last property in particular which points to the desirability of complexes of 1,2-alkeneditelluroate (1,2-alkeneditelluride, ditellurene) ligands.

Research on tetrathia- and tetraselenafulvalenes⁵ has evolved in parallel with work on metal dithiolenes and diselenenes. Recent work has resulted in the syntheses of the first examples of tetratellurafulvalenes.^{6,7} This paper describes the extension of these synthetic advances leading to the preparation of transition-metal ditellurene complexes.

Results and Discussion

Solutions of dilithium 1,2-benzeneditelluride, prepared in two steps from the phenylmercury hexamer⁸ according to Cowan,⁷ were found to react at room temperature with $\text{cis-PtCl}_2(\text{PPh}_3)_2$ to afford dark red-orange solutions from which orange air-stable crystals of $\text{Pt}(\text{Te}_2\text{C}_6\text{H}_4)(\text{PPh}_3)_2$ (**1**) could be isolated. Compound



1 was characterized by mass spectrometry as well as ^1H and ^{31}P

(1) For a recent compilation of leading references, see: Alvarez, S.; Vicente, R.; Hoffmann, R. *J. Am. Chem. Soc.* **1985**, *107*, 6253.

(2) (a) Bolinger, C. M.; Rauchfuss, T. B. *Inorg. Chem.* **1982**, *21*, 3947. (b) Gautheron, B.; Tainturier, G.; Pouly, S.; Théobald, F.; Vivier, H.; Laarif, A. *Organometallics* **1984**, *3*, 1495. (c) Sandman, D. J.; Stark, J. C.; Acampora, L. A.; Samuelson, L. A.; Allen, G. W.; Jansen, S.; Jones, M. T.; Foxman, B. M. *Mol. Cryst. Liq. Cryst.* **1984**, *107*, 1. These authors also allude to an attempt to prepare complexes of 1,2- $\text{C}_6\text{H}_4\text{Te}_2^{2-}$. (d) Wudl, F.; Zellers, E. T.; Cox, S. D. *Inorg. Chem.* **1985**, *24*, 2864.

(3) *Extended Linear Chain Compounds*; Miller, J. S., Ed.; Plenum: New York, 1982.

(4) (a) Kobayashi, A.; Sasaki, Y.; Kobayashi, H.; Underhill, A. E.; Ahmad, M. M. *J. Chem. Soc., Chem. Commun.* **1982**, 390. Kobayashi, A.; Sasaki, Y.; Kobayashi, Y.; Underhill, A. E.; Ahmad, M. M. *Chem. Lett.* **1984**, 305. (b) Bousseau, M.; Valade, L.; Legros, J.-P.; Cassoux, P.; Garbauskas, M.; Interrante, L. V. *J. Am. Chem. Soc.* **1986**, *108*, 1908. (c) Heuer, W. B.; Hoffman, B. M. *J. Chem. Soc. Chem. Commun.* **1986**, 174.

(5) Cowan, D. O.; Wiygul, F. M. *Chem. Eng. News* **1986**, *64*(29), 28.

(6) Wudl, F.; Aharon-Shalom, E. *J. Am. Chem. Soc.* **1982**, *104*, 1154.

(7) Lerstrup, K.; Talham, D.; Bloch, A.; Poehler, T.; Cowan, D. *J. Chem. Soc., Chem. Commun.* **1982**, 336.

(8) Winkler, H. J. S.; Wittig, G. *J. Organomet. Chem.*, **1963**, *28*, 1733.

[†]University of Illinois at Urbana-Champaign.

^{*}University of Delaware.